Shape effect on a single-nanoparticle-based plasmonic nanosensor

2013 Nanotechnology 24 285502

(http://iopscience.iop.org/0957-4484/24/28/285502)

Nanotechnology **24** (2013) 285502 (8pp) doi:10.1088/0957-4484/24/28/285502

Shape effect on a single-nanoparticle-based plasmonic nanosensor

Hongming Shen[1], Guowei Lu[1], Tianyue Zhang[1], Jie Liu[1], Ying Gu[1], Pascal Perriat[2], Matteo Martini[3], Olivier Tillement[3] and Qihuang Gong[1]

[1] State Key Laboratory for Mesoscopic Physics, Department of Physics, Peking University, Beijing 100871, People's Republic of China
[2] MATEIS, UMR 5510 CNRS, INSA-Lyon, Université de Lyon, 20 avenue Albert Einstein, F-69621 Villeurbanne Cedex, France
[3] LPCML, Université de Lyon, Université Claude Bernard, 43 Bd du 11 novembre 1918, F-69622 Villeurbanne Cedex, France

E-mail: guowei.lu@pku.edu.cn and qhgong@pku.edu.cn

Received 2 April 2013, in final form 17 May 2013
Published 21 June 2013
Online at stacks.iop.org/Nano/24/285502

Abstract
Plasmonic refractometric nanosensors based on single nanostructures, i.e. spherical, nanorod- and bipyramid-shaped gold nanoparticles, are investigated and compared numerically by employing the finite-difference time-domain method. The results show that the plasmonic sensing ability is distributed anisotropically around the nanorod and bipyramid, even for spherical nanoparticles when the illumination light is linearly polarized. To optimize nanosensor performance, some anisotropy in the shape of nanoparticles is required, this latter serving as an intrinsic light polarization filter to suppress the disturbance from localized surface plasmon resonance in other directions. The plasmonic near-field can be engineered by controlling the shape to achieve a concentrated and localized electromagnetic field, in direct relation with the sensing ability. Taking these factors into account, the gold bipyramid nanoconstruct which is easily available in experiment is proposed as an efficient plasmonic sensing platform. The bipyramid presents both highly localized sensitivity and high scattering cross-section, thus avoiding the trade-off during the selection of the widely used nanorod-shaped sensors. The parameters of the bipyramid structure can be optimized by numerical simulation to improve the plasmonic sensing. Our findings permit a deeper understanding of single-nanoparticle-sensor behavior, and the study provides an opportunity to optimize the plasmonic sensor.

(Some figures may appear in colour only in the online journal)

1. Introduction

A surface plasmon is kind of polariton, i.e. a photon coupled to an electron, such that either photons or electrons can be used to excite the electron oscillation [1–3]. Interest in surface plasmons is driven by the unique and novel properties of nanoscale materials such as the strong interaction of metal particles with light. Label-free nanoscale sensors based on plasmonic nanostructures, as one of many novel and potential applications, are attracting increasing attention for the optical sensing of chemical and biological analytes [4, 5]. Specifically, the plasmonic-based refractometric sensors exploit the phenomenon of localized surface plasmon resonance (LSPR) which transduces molecular binding events at their surface into macroscopically measurable optical signals, since the LSPR frequency of the metallic nanostructure is a function of the local environment refractive index (RI). This approach to label-free sensing, in the beginning proposed for ensemble colloids in suspension [6, 7], was then demonstrated for immobilized nanoparticles on a transparent substrate [8] and was recently extended to the limit of single plasmonic nanoparticles [9–14].

Single-nanoparticle-based plasmonic sensors enable higher spatial resolution in multiplexed assays and permit the detection of a reduced number of molecules when integrated with microfluidic techniques [4, 15]. Single plasmonic nanoparticles usually present narrow resonance bandwidths compared to the ensemble colloids. In addition, single nanoparticles have promising applications for more flexible measurements in solution, even inside cells and tissues where the fixed large plasmonic arrays are normally unable to penetrate. Biomolecular recognition was firstly reported using light scattering of a single gold nanoparticle functionalized with biotin, spectral shifts as small as 2 meV being detected due to 1 μM streptavidin specific binding [9]. Later, LSPR shift due to streptavidin concentration as low as 100 pM was observed upon incubation of a single biotin-functionalized gold nanorod [16], which presented obvious higher sensitivity than the gold sphere-like nanoparticles. Plasmonic biosensors based on a single nanoparticle in an optimized design experiment could respond specifically to the binding of a few biological molecules, even to a single biological macromolecule in theory [17]. By miniaturizing the sensor down to a single plasmonic nanoparticle, the sensitivity volume of the detection system is reduced to a size-scale commensurate with the size of biomolecular analytes, rendering it possible to detect single unlabeled molecule.

Single binding events of nanoparticle-labeled DNA strands were detected with LSPR measurement of a single 100 nm gold particle. In that study the scattering signal was enhanced by a 20 nm gold particle as label [14]. Later, unlabeled molecule detection of individual molecules was demonstrated to the ultimate sensing limit by Hafner *et al* by monitoring antibody–antigen unbinding events through the scattering spectra of individual gold bipyramids [18]. The bipyramid nanostructure was found to yield higher sensitivity than nanorods and nanospheres in the ensemble experiments [19]. Although much experimental and theoretical effort has been devoted to the understanding of the nanosensors, it remains inadequate for rational design and optimization. Recently, a sensitive (∼700 times higher than plasmon scattering sensors) assay-method-based photothermal microscopy was reported by Orrit *et al* using a single gold nanorod to detect single unlabeled molecules [20]. Nevertheless, the plasmonic-nanosensor-based optical scattering is more feasible for the applications in practice. Interestingly, Ament *et al* recently also demonstrated experimentally that a single protein could be detected based on conventional optical scattering. They adopted an intense white light laser source and an intensified CCD camera detector to increase the signal to noise ratio greatly [21]. However, the protein molecule used in their experiments is a large biological molecule, i.e. a blood plasma protein fibronectin with a molecular weight of 450 kDa. To detect a smaller molecule based on optical scattering, the detection limit must be optimized further. Apart from the improvements of optical source and detectors, we propose to rationally select plasmonic geometry to optimize nanoparticle-based sensors.

In this study, basic rules on how to optimize single-particle-based plasmonic nanosensor are demonstrated by theoretically studying the plasmonic sensing behaviors of spherical, nanorod- and bipyramid-shaped nanoparticles. The plasmonic sensing ability is distributed anisotropically along the plasmonic nanoparticle, even for a spherical symmetrical nanoparticle under linearly polarized illumination. Some anisotropy in the shape of the plasmonic nanoparticle is required to optimize single-nanoparticle-based sensors in practical applications. Highly concentrated and small plasmonic near-field volume at a sharp apex usually results in a large LSPR shift response due to the molecule binding. Taking these factors into account, the gold bipyramid nanoconstruct presents both highly localized sensitivity and high scattering cross-section, which also avoids the trade-off during the selection of the nanorod-shaped sensors.

2. Methods

In order to investigate the plasmonic sensing abilities of individual gold nanoparticles (with a spherical, nanorod or bipyramid shape), the finite-difference time-domain (FDTD) method is used to calculate the LSPR characteristics of individual nanostructures [22, 23]. The FDTD method is simply a space and time discretization of the Maxwell curl equations, i.e. the Yee algorithm. An arbitrary construct of the objective can be simulated on the Yee mesh. The FDTD method has been extensively employed to study both the near- and far-field electromagnetic responses of metal nanostructures. The method is a powerful computational technique which is widely used to calculate the optical properties of nanostructures. Such a method permits the computation of (i) the electromagnetic field distribution of the nanostructure surroundings and (ii) the absorption and scattering cross-sections of metallic nanostructures. In particular, the FDTD method can provide a full spectrum in a single simulation by propagating a short pulse in the time-domain. The optical dielectric function of the gold material is modeled using a Drude–Lorentz dispersion function. The refractive index of the surrounding media is taken to be 1.33 for water in all simulations and the refractive index of silica glass is 1.49. In calculations, the nanoparticle is a gold sphere with diameter 40 nm. The half-bipyramid is drawn as circular cones with an apex angle of 36° (base diameter of 32 nm, top diameter of 10 nm, capped with a tangential spheroidal surface, the total height for the bipyramid being 98 nm). The conical and spheroidal geometries are joined in such a way that both the resulting surface and its first derivative are continuous. It should be noted that the bipyramidal shape is controllable during wet chemical synthesis procedures [18, 19, 24]. The LSPR properties of gold nanorods are also calculated for comparison, the structures being that of a cylinder with two semispherical caps. In this paper, two samples of gold nanorods (rod-10–40 with diameter of 10 nm and total length of 40 nm and rod-30–102 with diameter of 30 nm and total length of 102 nm) are calculated and compared in detail.

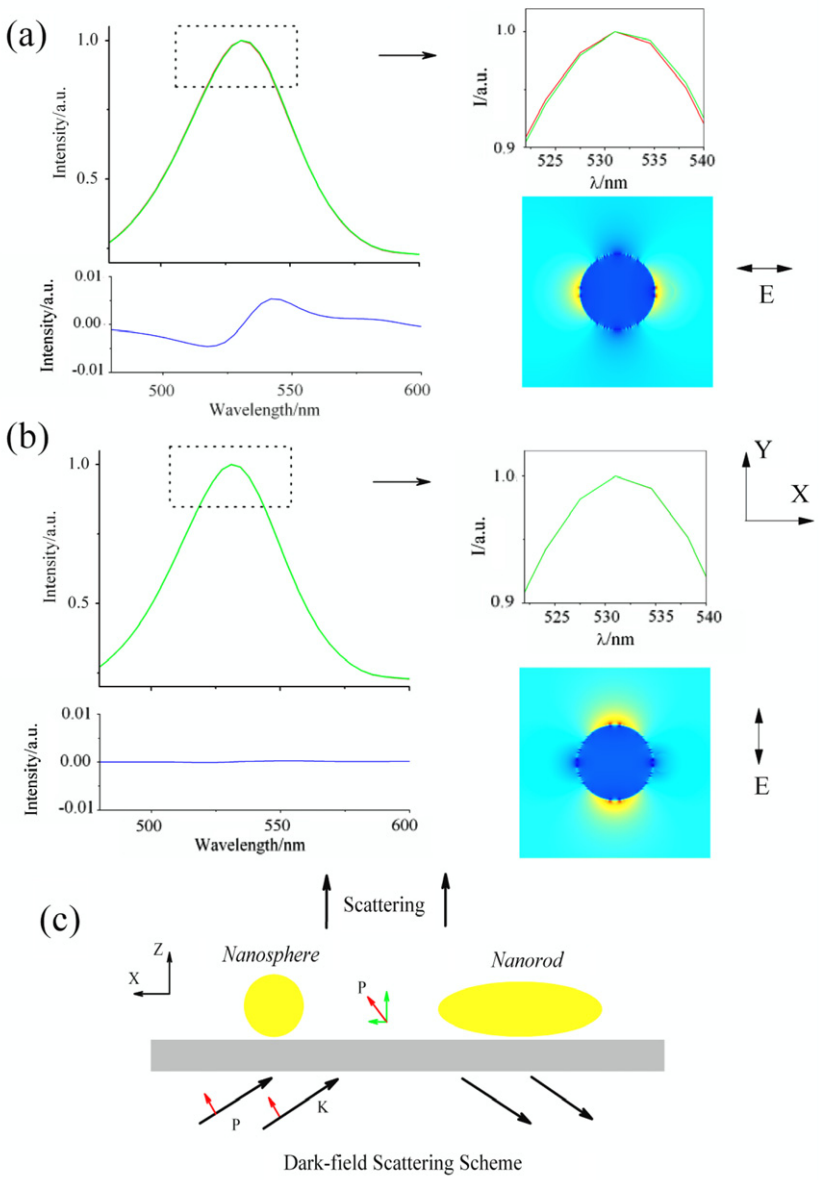

Figure 1. LSPR spectra and electromagnetic near-field distributions of a spherical gold nanoparticle with a diameter of 40 nm illuminated with a planar continuous wave of (a) for polarization along the *x* direction and (b) along the *y* direction. A dielectric particle with a diameter of 10 nm was placed at the right of the nanoparticle along the direction to simulate the binding event. The spectral differences (in blue) and the enlarged regions are plotted correspondingly to clarify the LSPR peak shift induced by the binding. The red and green curves are the LSPR peaks before and after binding separately. (c) Plasmonic sensing scheme based on the dark-field scattering of the nanoparticles.

3. Results and discussion

As for the highly symmetrical spherical nanoparticles, the LSPR response to a dielectric sphere is calculated under different linearly polarized plane waves. The dielectric sphere with a diameter of 10 nm and a refractive index of $n = 1.57$ representing a binding molecule is placed in the vicinity of the gold nanoparticle on the x axis. The illumination light propagates along the z direction with linear polarizations in the x or y direction respectively. The extinction spectra of the gold nanoparticles are calculated with or without the dielectric sphere to reveal the LSPR response to the molecule bonding events. The electric field distribution of the cross-sectional plane ($z = 0$) is shown in figure 1 under illumination light at the frequency of the LSPR peak. Interestingly, the LSPR peak definitely presents a red-shift due to the presence of the dielectric sphere when the illumination light polarizes along the x direction. This shift is absent if the illumination light polarization is along the y direction. Thus, the distribution of the sensing ability is also anisotropic even for spherical nanoparticles under linearly polarized illumination. It seems that the effect of the dielectric sphere on the LSPR mode is more significant at the position where the plasmonic near-field is stronger, which results in a strong interaction between the light and matter. The plasmonic near-field is distributed with a maximum along the illumination light polarization.

Hence, the sensing objective should be docked at the position with high near-field intensity for a large LSPR shift. These results imply that the plasmonic near-field distribution is certainly the key factor to determine the interaction between the LSPR mode and the molecule [14]. From our previous study [17], plasmonic nanosensors based on gold nanorods present an anisotropic distribution of the sensing ability in the radial direction and also along the surface. Specifically, the sensitivities are higher at both hemispherical ends of the nanorod apex. Here, the plasmonic near-field pattern of the single sphere particle is determined mainly by the excitation of the illumination light. Hence, the polarization of the illumination light has to be considered carefully while performing the plasmonic sensing.

The dark-field scattering method is often utilized to realize the single-nanoparticle-based plasmonic sensing [5, 9, 10, 15]. In dark-field measurements, the sample is illuminated with a high angle by annular incidence or evanescent near-field excitation and only the scattered light by the nanostructure is collected for imaging by the objective lens and guided to the spectrometer to obtain an optical spectrum. Hence, the illumination of the white light source usually is not an ideal linear polarization plane wave in practical dark-field experiments. Such light polarization would decrease the sensing signal to noise ratio (S/N) of a plasmonic-sensor-based spherical nanoparticle. For instance, an incident light with p-polarization can be decomposed into the x and z direction under dark-field configurations, which invoke electrons oscillating in both directions as indicated in figure 1(c). If a dielectric sphere is placed on the x axis near the nanoparticle, the light scattering of the nanoparticle would contain the information related to LSPR in both directions, i.e. the scattering signal excited by the light polarized in the x and z direction simultaneously. For the spherical nanoparticles, the LSPR modes in the x and z direction are almost identical, so that the total scattering signal would only present a slight broad peak. In this situation, the LSPR shift cannot be extracted easily. On the contrary, for nanorod shapes, the LSPR frequencies in the x and z direction are distinctly separated. The transversal LSPR mode should not disturb the response of the longitudinal LSPR mode to the molecule bonding which is often utilized for plasmonic sensing applications. Hence, some anisotropy in the shape of the nanoparticles can serve as an intrinsic light polarization filter to suppress the disturbance, brought by other LSPR modes, of the nanoparticle itself. The anisotropic shape can also tune the LSPR peak to longer wavelengths which usually results in higher bulk sensitivity. In an alternative view of the phenomenon, the nanorod intrinsically responds to the molecule bonding events by an LSPR mode that oscillates only in one dimension, while the scattering of a spherical nanoparticle comes from the superimposed LSPR modes in two or three dimensions. To extend this concept, an LSPR mode concentrated into zero dimensions (a hot spot) would result in a better sensitivity. For instance, the electromagnetic field can be further concentrated within the gap of coupled nanoparticles, permitting a more sensitive response to invasive molecules. This has already been demonstrated in a previous study [17, 25]. The hot gap of coupled nanostructures is beyond the scope of the current study so that in this paper we only focus on single-nanoparticle-based plasmonic sensors.

Now, nanorod-shaped gold nanoparticles are generally used for single-nanoparticle-based plasmonic nanosensors due to their obvious advantages over spherical nanoparticles. However, to achieve high sensitivity performance of the nanorods, there is usually a trade-off between the signal intensity and binding induced shift of the nanorods' dark-field scattering spectra [16, 17, 21, 26]. We could be tempted to choose the smallest possible nanorod because of the higher LSPR local sensitivity near the surface and the narrower full width at half maximum (FWHM) of the LSPR band. However, small nanorods exhibit small scattering cross-sections under dark-field illumination which decreases the signal intensity and limits the accuracy needed to determine the plasmon resonance maximum [17–19]. According to the above discussions, gold bipyramid nanoconstructs are proposed here instead of nanorods to achieve highly localized sensing. The bipyramid architecture helps to avoid the trade-off problem of the nanorods. Because the scattering signal would be high when using a large size bipyramid, at the same time, the nano-bipyramid provides high local sensitivity due to its sharp apex shape. The molecules binding at close proximity becomes more obvious due to high plasmonic near-field at the apex, leading to a large shift of LSPR. Additionally, gold bipyramids can be easily fabricated and the bipyramidal shape is perfectly controllable during wet chemical synthesis procedures [18, 19, 24, 27], which provides a potential opportunity to improve the sensitivity of single-nanoparticle sensors. To demonstrate the advantage of bipyramid-shaped nanosensors, the optical properties of the rod-10–40, rod-30–102 and the bipyramid (as shown schematically in figure 2) are calculated and compared in detail.

As known, the detection limit (L_{M}) of a single-nanoparticle sensor is given by the relation [16, 17]:

$$L_M = \frac{1}{V_{\mathrm{A}} \cdot \Delta n} \frac{V_{\mathrm{sens}}}{3S_{\mathrm{bulk}}} \frac{\sqrt{\sigma_{\mathrm{sys}}^2 + \sigma_{\mathrm{sig}}^2}}{\exp\left[-\frac{2r}{D_{\mathrm{decay}}}\right]}, \qquad (1)$$

$$\sigma_{\mathrm{sig}} = \frac{1}{4.7} \frac{\mathrm{FWHM}}{\sqrt{A \cdot C_{\mathrm{sca}}}}$$

V_{A} is the volume of the analyte molecule, Δn the difference between the refractive index (RI) of the analyte and that of the surrounding medium and r the separation distance of the analyte from the nanostructure surface (the anisotropic distribution of the sensing ability will be discussed below). These three factors simply describe how the analyte influences the LSPR response. σ_{sys} is the uncertainty due to the detection system (arising mainly from physical system stability such as the microscope focus and sample stage drift). A is a constant that accounts for the input photon flux, the integration time and the quantum efficiency of the measurement system. These two factors present the influence of the detection system. The nanostructure is characterized by five parameters: S_{bulk} (the bulk RI sensitivity), V_{sens} (the

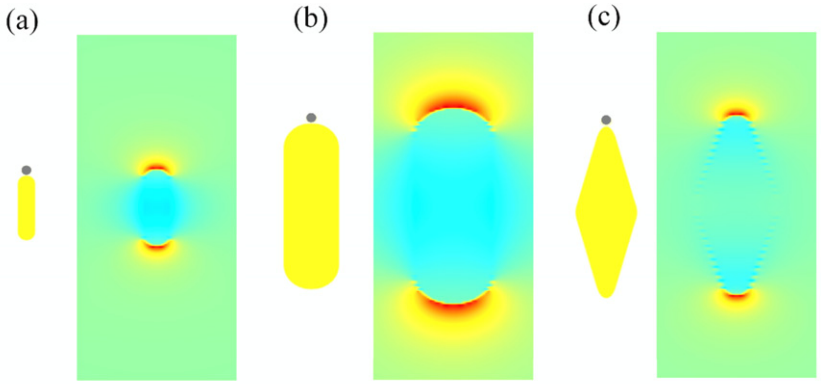

Figure 2. Geometrical schemes of rod-10–40, rod-30–102 and the bipyramid in the presence of a dielectric sphere and electromagnetic near-field distributions of the nanostructures illuminated with a planar continuous wave.

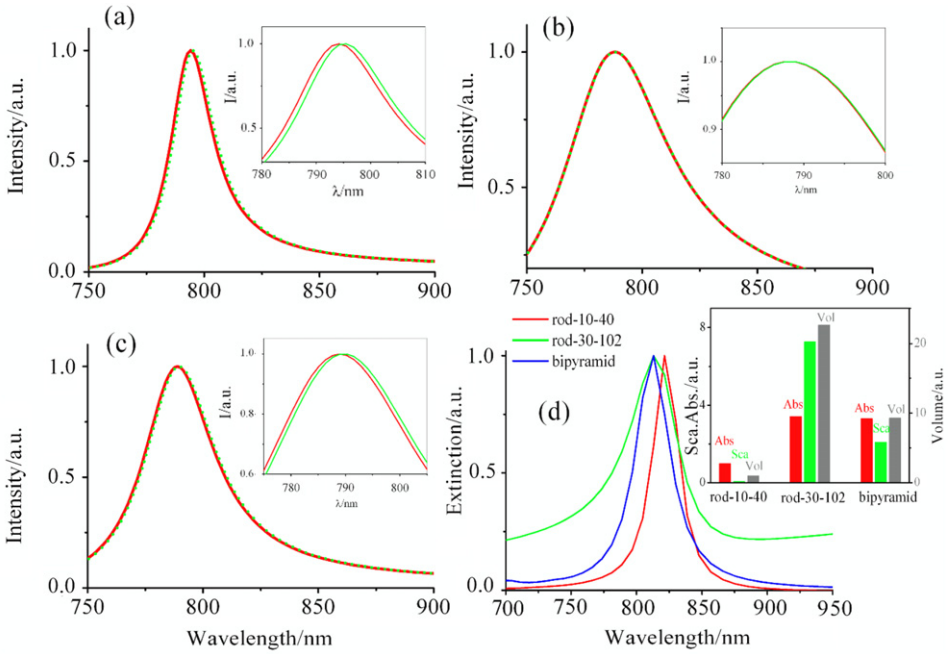

Figure 3. Red-shift of the LSPR peak of rod-10–40 (a), rod-30–102 (b) and the bipyramid (c) induced by a dielectric sphere with a radius of 3 nm and a refractive index of 1.57; the refractive index of the surrounding media is 1.33. In the inset, the enlarged figures permit us to view the red-shift brought by the presence of the dielectric sphere. (d) Normalized LSPR extinction spectra (sum of the scattering and absorption) of rod-10–40 (red), rod-30–102 (green) and the bipyramid (blue). The inset presents the scattering and absorption coefficients at the resonance (all normalized to the scattering of rod-10–40). The normalized volumes of the nanostructures are also presented for comparison.

total sensing volume of the nanostructure), D_{decay} (the decay length of the sensing ability), FWHM and C_{sca} (the scattering cross-section). These five parameters provide the clues to design an optimized nanostructured plasmonic sensor, i.e. an optimized nanoparticle should have large S_{bulk} and C_{sca}, but small FWHM, V_{sens} and D_{decay} for a high sensitivity.

Three nanostructures selected in this study all present longitudinal LSPR peaks at $\sim\lambda = 820$ nm. The bulk RI sensitivity S_{bulk} of nanoparticles can be predicted from the wavelength of the LSPR peak [28]. After appropriate calculations discussed below, the S_{bulk} values of the three nanostructures are similar with values around 450 nm/RIU (refractive index unit). To find this result three-dimensional FDTD simulations are first executed to calculate the scattering and absorption cross-sections of the nanostructures. The extinction spectra (the sum of absorption and scattering) are shown in figure 3(d). The LSPRs' FWHM of rod-10–40, rod-30–102 and the bipyramid are about 23 nm, 48 nm and 32 nm respectively. The scattering and absorption coefficients at resonance (all normalized to the absorption cross-section of rod-10–40) are shown in figure 3. The volumes of the nanostructures, normalized to that of rod-10–40, are also presented in the inset of figure 3(d) for comparison. For small size (rod-10–40), the scattering coefficient is only about 0.07 of its absorption coefficient, which is not really suitable for sensing applications based on optical scattering measurements. As the volume increases, the relative scattering coefficient of rod-30–102 grows by more than two orders

of magnitude. This is the reason why large nanorods are widely used in current plasmonic sensing applications. For instance, in two recent state-of-the-art works about high sensitivity nanosensors, the size of optimized nanorods in optical scattering measurements [21] is larger than that of the optimized nanorods used in photothermal assay [20]. However, the researchers fall into the temptation of choosing the smallest possible nanorod because of the higher LSPR local sensitivity. If the physical and sensing volumes are large, then the sensitivity to the presence of small molecules is decreased. Here, the bipyramid has a length comparable to that of the rod-30–102 but is thinner. Calculations show that the scattering coefficient of the bipyramid is about half of the rod-30–102 but is still detectable efficiently. In contrast, the scattering signal of the small rod-10–40 is weak. It only works well in the photothermal assay where the absorption cross-section is concerned [20]. In fact, when taking into account both the LSPR FWHM and the scattering coefficient, the σ_{sig} values of the rod-30–102 and the bipyramid are almost comparable. Therefore, the bipyramid presents a comparable uncertainty of the scattering signal to that of the large size nanorod.

To investigate the local sensing ability of the three nanostructures, the binding of a single biological molecule onto the sensor surface is simply simulated by placing a dielectric sphere near the nanostructures. The sensitivity distribution of a nanorod sensor is not isotropic [16, 17], but is higher at the hemispherical ends due to the strong near-field induced at this location. The choice of a dielectric sphere with a radius of 3 nm and a refractive index of $n = 1.57$ corresponds to a common model of the streptavidin molecule. In practice, with the help of specific surface treatment, the analytes can be precisely grafted onto the highest sensitivity area [20, 29]. To simulate this experiment, the dielectric sphere is placed near the apex end of the nanorods or bipyramids in calculations. This process has been experimentally realized (i) for the detection of a single molecule by surface enhanced Raman scattering [29] and (ii) to prove the sensitivity of a photothermal assay [20]. The LSPR peak red-shift induced by the presence of the dielectric sphere is shown in figure 3. For rod-10–40, rod-30–102 and the bipyramid, they are of about 1.0 nm, 0.1 nm and 0.9 nm respectively. The result of rod-10–40 is in good agreement with a recent report that a single nanorod with a diameter of 9 nm can be used in a photothermal assay to detect successfully a single non-absorbing streptavidin with a molecular weight of ~53 kDa [20]. As can be seen, the localized sensing ability of the bipyramid is comparable to that of rod-10–40, so that single bipyramids should be good platforms for plasmonic sensors with highly localized sensitivity. In fact, the bipyramid presents a scattering signal comparable to that of the large nanorod and a local sensitivity comparable to that of the small nanorod. Hence the bipyramid would avoid the trade-off problem by using the nanorod shape for single-nanoparticle sensing, which significantly improves the sensor performance based on optical scattering and also benefits the photothermal assay with such a nanostructure.

To provide valuable insight into the LSPR response, the LSPR spectra of the nanostructures immersed in a different environmental index are calculated to obtain their bulk sensitivity. And the spectra of the nanostructures coated by different thickness silica layers are also evaluated to characterize their sensitivity simply from the decay length. Typical results are shown in figure 4. The bulk sensitivities S_{bulk} of rod-10–40, rod-30–102 and the bipyramid are 454, 461 and 445 nm/RI unit respectively. Because the LSPR peaks are almost the same, it can be concluded that the bulk sensitivities of nanoparticles depend on the wavelength of the LSPR peak [17, 30]. However the local sensitivity distribution around the plasmonic sensor is anisotropic and strongly dependent on the shape, the size and the configuration of the nanostructures. As can be seen from figure 4(b), the LSPR peak shifts towards the red as the coating layer thickness increases. The red-shift can be correctly fitted by the equation: $\lambda_{LSPR} = \lambda_0 + S_{bulk} \cdot \Delta n \cdot (1 - e^{-2r/D_{decay}})$ [16]. In the case of rod-10–40 and the bipyramid, the D_{decay} is short, so that the localized sensing ability is suitable for small molecule detection. For the nanorod-30–102, the sensitivity is lower which corresponds to large D_{decay} and the possibility of measuring more target molecules' binding events for a large dynamic response range.

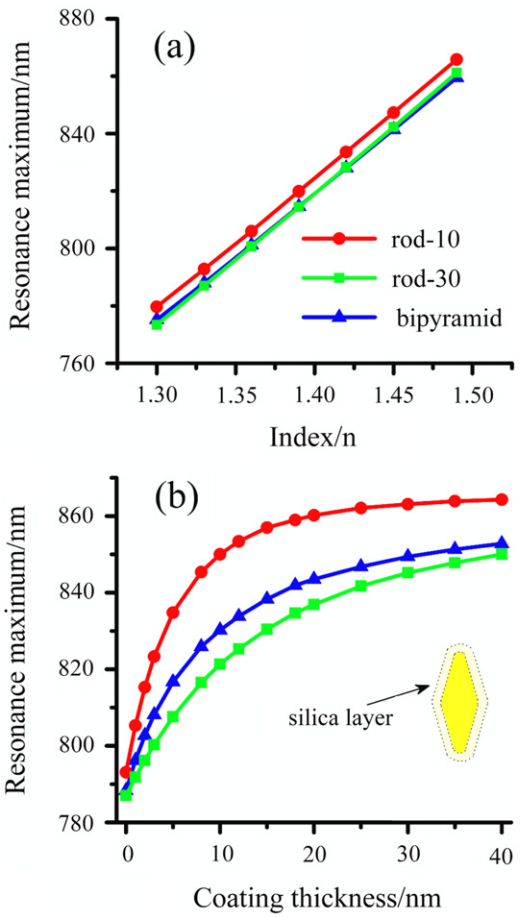

Figure 4. (a) LSPR peak maxima of the nanostructures in environments with various refractive indices n and (b) LSPR peak maxima of the nanostructures coated with different thickness silica layers in water. The data dots are fitted correspondingly to obtain the bulk sensitivity and sensitivity decay length.

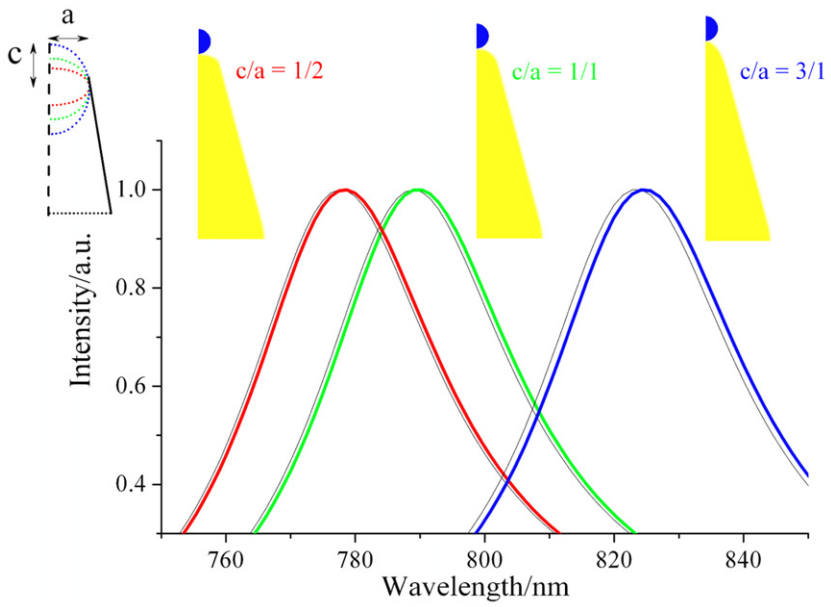

Figure 5. LSPR spectra of the bipyramids with different apex shape in the presence of a dielectric sphere (the LSPR spectra in the absence of the sphere are also calculated and are shown as black solid lines). The radius ratios of the different spheroid apex ends are indicated in the scheme (top left).

To better understand this anisotropic effect, the electromagnetic near-field distributions around the nanostructures have been calculated and are shown in figure 2. The calculations of the field distribution are performed under illumination by a planar continuous light at resonant frequencies. As can be seen from figure 2, the near-field distribution volume of the nanorod-30–102 is the largest one, whereas those of the small size rod-10–40 and the bipyramid are almost equivalent. This is in agreement with the fact that the electromagnetic field in the vicinity of sharp curvatures usually exhibits subwavelength confinement of light [31–33]. The magnitude of the LSPR shift is related to the perturbation of the electromagnetic near-field induced by the local change of the refractive index. Then for a dielectric sphere with a given volume, the bipyramid and small nanorod that possesses the smallest spatial extension of the electromagnetic near-field should present the larger LSPR red-shift. Inspired by the relation between the local sensitivity and the near-field distribution, the apex shape of the bipyramid is varied as indicated in figure 5 to evaluate the shape dependence of the plasmonic localized sensitivity. All parameters of the bipyramid architecture are maintained except the apex end: the sharp curvatures of the bipyramid apex are then adjusted by tuning the ratio of the spheroidal shape's radii (the geometry $c/a = 1/1$ is just equivalent to a spherical apex end). The LSPR spectra of the bipyramids with different apex shapes are calculated (i) in the absence and (ii) in the presence of the dielectric sphere, as shown in figure 5. The LSPR red-shifts induced by the dielectric sphere are of 0.7 nm, 0.9 nm and 1.2 nm for the case of $c/a = 1/2, 1/1$ and $3/1$ respectively. Moreover, the bulk sensitivity was also calculated for these bipyramids with different apex shapes, giving values of 431, 445 and 478 nm/RIU respectively. This change can be explained by the slight increase in the length of the bipyramids following the c/a modification. Then, the LSPR red-shift induced by the dielectric sphere for the bipyramid with $c/a = 3/1$ increases by about 70% (from 0.7 to 1.2 nm) compared to the bipyramid with $c/a = 1/2$, whereas the bulk sensitivity increases by only about 11% (from 431 to 478 nm/RI unit). The red-shift is thus due to the sharper curvature of the bipyramid structure, which permits a larger field enhancement near the apex end and presents a short sensitivity decay length. All the results demonstrate that the localized sensitivity of the bipyramid is strongly dependent on the apex shape. An optimization of this parameter provides an opportunity to design plasmonic sensors for single-molecule detection.

4. Conclusions

In summary, plasmonic sensors based on single gold nanostructures (spherical, nanorod- and bipyramid-shaped nanoparticles) are investigated and compared theoretically by employing the FDTD method. The plasmonic sensing ability is distributed anisotropically even for a spherically symmetrical nanoparticle when the illumination light is linearly polarized. Some anisotropy in the shape of the nanoparticle is required to optimize the sensor in practical applications, the anisotropic particle then serving as an intrinsic light polarization filter to increase the signal noise ratio. The plasmonic sensitivity is highly related to the localized plasmonic near-field which can be tuned by the nanostructure shape. Taking these factors into account, the gold bipyramid nanoconstruct is evidenced to be an efficient plasmonic nanosensor platform. The bipyramid presents both highly localized sensitivity and high scattering cross-section, which also avoids the trade-off during the selection of the nanorod-shaped sensor. Moreover, the parameters of the

bipyramid structure can be optimized, as demonstrated by numerical simulation, to improve the sensing performance, and our findings permit a deeper understanding of single-plasmonic-nanoparticle-based nanosensors.

Acknowledgments

This work was supported by the National Key Basic Research Program of China (grant no. 2013CB328703) and the National Natural Science Foundation of China (grant nos 61008026, 11121091, 90921008).

References

[1] Bohren C F and Huffman D R 1983 *Absorption and Scattering of Light by Small Particles* (New York: Wiley)
[2] Maier S A 2007 *Plasmonics: Fundamentals and Applications* (New York: Springer)
[3] Kreibig U and Vollmer M 1995 *Optical Properties of Metal Clusters* (Berlin: Springer)
[4] Anker J N, Hall W P, Lyandres O, Shah N C, Zhao J and Van Duyne R P 2008 Biosensing with plasmonic nanosensors *Nature Mater.* **7** 442–53
[5] van Dijk M A, Tchebotareva A L, Orrit M, Lippitz M, Berciaud S, Lasne D, Cognet L and Lounis B 2006 Absorption and scattering microscopy of single metal nanoparticles *Phys. Chem. Chem. Phys.* **8** 3486–95
[6] Elghanian R, Storhoff J J, Mucic R C, Letsinger R L and Mirkin C A 1997 Selective colorimetric detection of polynucleotides based on the distance-dependent optical properties of gold nanoparticles *Science* **277** 1078–81
[7] Englebienne P 1998 Use of colloidal gold surface plasmon resonance peak shift to infer affinity constants from the interactions between protein antigens and antibodies specific for single or multiple epitopes *Analyst* **123** 1599–603
[8] Frederix F, Friedt J, Choi K, Laureyn W, Campitelli A, Mondelaers D, Maes G and Borghs G 2003 Biosensing based on light absorption of nanoscaled gold and silver particles *Anal. Chem.* **75** 6894–900
[9] Raschke G, Kowarik S, Franzl T, Sönnichsen C, Klar T A, Feldmann J, Nichtl A and Kürzinger K 2003 Biomolecular recognition based on single gold nanoparticle light scattering *Nano Lett.* **3** 935–8
[10] McFarland A D and Van Duyne R P 2003 Single silver nanoparticles as real-time optical sensors with zeptomole sensitivity *Nano Lett.* **3** 1057–62
[11] Rindzevicius T, Alaverdyan Y, Dahlin A, Höök F, Sutherland D S and Käll M 2005 Plasmonic sensing characteristics of single nanometric holes *Nano Lett.* **5** 2335–9
[12] van Dijk M A, Lippitz M and Orrit M 2005 Far-field optical microscopy of single metal nanoparticles *Acc. Chem. Res.* **38** 594–601
[13] Sherry L J, Jin R, Mirkin C A, Schatz G C and Van Duyne R P 2006 Localized surface plasmon resonance spectroscopy of single silver triangular nanoprisms *Nano Lett.* **6** 2060–5
[14] Sannomiya T, Hafner C and Voros J 2008 *In situ* sensing of single binding events by localized surface plasmon resonance *Nano Lett.* **8** 3450–5
[15] Sannomiya T and Vörös J 2011 Single plasmonic nanoparticles for biosensing *Trends Biotechnol.* **29** 343–51
[16] Nusz G J, Curry A C, Marinakos S M, Wax A and Chilkoti A 2009 Rational selection of gold nanorod geometry for label-free plasmonic biosensors *ACS Nano* **3** 795–806
[17] Lu G, Hou L, Zhang T, Li W, Liu J, Perriat P and Gong Q 2011 Anisotropic plasmonic sensing of individual or coupled gold nanorods *J. Phys. Chem.* C **115** 22877–85
[18] Mayer K M, Hao F, Lee S, Nordlander P and Hafner J H 2010 A single molecule immunoassay by localized surface plasmon resonance *Nanotechnology* **21** 255503
[19] Lee S, Mayer K M and Hafner J H 2009 Improved localized surface plasmon resonance immunoassay with gold bipyramid substrates *Anal. Chem.* **81** 4450–5
[20] Zijlstra P, Paulo P M R and Orrit M 2012 Optical detection of single non-absorbing molecules using the surface plasmon resonance of a gold nanorod *Nature Nanotechnol.* **7** 379–82
[21] Ament I, Prasad J, Henkel A, Schmachtel S and Sönnichsen C 2012 Single unlabeled protein detection on individual plasmonic nanoparticles *Nano Lett.* **12** 1092–5
[22] Taflove A and Hagness S C 2005 *Computational Electrodynamics: The Finite-Difference Time-Domain Method* 3rd edn (Norwood, MA: Artech House)
[23] Oskooi A F, Roundy D, Ibanescu M, Bermel P, Joannopoulos J D and Johnson S G 2010 Meep: a flexible free-software package for electromagnetic simulations by the FDTD method *Comput. Phys. Comm.* **181** 687–702
[24] Liu M Z and Guyot-Sionnest P 2005 Mechanism of silver(I)-assisted growth of gold nanorods and bipyramids *J. Phys. Chem.* B **109** 22192–200
[25] Acimovic S S, Kreuzer M P, González M U and Quidant R 2009 Plasmon near-field coupling in metal dimers as a step toward single-molecule sensing *ACS Nano* **3** 1231–7
[26] Nusz G J, Marinakos S M, Curry A C, Dahlin A, Hook F, Wax A and Chilkoti A 2008 Label-free plasmonic detection of biomolecular binding by a single gold nanorod *Anal. Chem.* **80** 984–9
[27] Kou X, Ni W, Tsung C K, Chan K, Lin H Q, Stucky G D and Wang J F 2007 Growth of gold bipyramids with improved yield and their curvature-directed oxidation *Small* **3** 2103–13
[28] Miller M M and Lazarides A A 2005 Sensitivity of metal nanoparticle surface plasmon resonance to the dielectric environment *J. Phys. Chem.* B **109** 21556–65
[29] Le Ru E C, Grand J, Sow I, Somerville W R C, Etchegoin P G, Treguer-Delapierre M, Charron G, Félidj N, Lévi G and Aubard J 2011 A scheme for detecting every single target molecule with surface-enhanced Raman spectroscopy *Nano Lett.* **11** 5013–9
[30] Sannomiya T, Hafner C and Voros J 2009 Shape-dependent sensitivity of single plasmonic nanoparticles for biosensing *J. Biomed. Opt.* **14** 064027
[31] Jain P K and El-Sayed M A 2008 Noble metal nanoparticle pairs: effect of medium for enhanced nanosensing *Nano Lett.* **8** 4347–52
[32] Schuller J A, Barnard E S, Cai W, Jun Y C, White J S and Brongersma M L 2010 Plasmonics for extreme light concentration and manipulation *Nature Mater.* **9** 193–204
[33] Jain P K and El-Sayed M A 2007 Surface plasmon resonance sensitivity of metal nanostructures: physical basis and universal scaling in metal nanoshells *J. Phys. Chem.* C **111** 17451–4